Supporting Information for

Non-linear relationships between air temperature and river water quality revealed by a panel dataset of 276 Chinese cities

Kehan Liang [a,1], Litiao Hu [a,1], Zongwei Ma [a,b,c*], Shenyuan Huang [a,d], Miaomiao Liu [a,c], Wen Fang [a,c], Jianxun Yang [a,c,d], Jun Bi [a,b,c]

a State Key Laboratory of Water Pollution Control and Green Resource Recycling, School of the Environment, Nanjing University, Nanjing, China.

b Jiangsu Collaborative Innovation Center of Atmospheric Environment and Equipment Technology (CICAEET), Nanjing University of Information Science & Technology, Nanjing, Jiangsu, China.

c Basic Science Center for Energy and Climate Change, Beijing, China

d Institute for the Environment and Health, Nanjing University, Suzhou Campus, Suzhou, China

1 These authors contributed equally.

* Corresponding authors: Zongwei Ma (zma@nju.edu.cn).

Contents of this file

Introduction

This document provides additional details about the impacts of air temperature on river water quality.

Supplementary Note 1. Quality-based water scarcity risks in historical period.

According to Environmental Quality Standards for Surface Water of China, the maximum water quality thresholds are based on COD_{Mn} and NH_3-N concentrations: COD_{Mn} = 6.0 mg/L, NH_3-N = 1.0 mg/L for domestic use; COD_{Mn} = 10.0 mg/L, NH_3-N = 1.5 mg/L for industrial use; COD_{Mn} = 15.0 mg/L, NH_3-N = 2 mg/L for agricultural use. These water quality parameter thresholds represent the minimum water quality requirements for specific industrial uses, and exceeding the thresholds requires additional water withdrawals for concentration dilution (van Vliet et al., 2017).

We incorporate quality requirements for city i, and first calculate the pollution risk of local water quality conditions for each water use sector, as shown in ***Eq. (S1)***.

$$\mathrm{WP}_{i,t} = \begin{cases} 0, & \mathrm{C}_{a,i,t} \le \mathrm{Cmax}_{a,j} \\ \sum\left(\dfrac{\mathrm{C}_{a,i,t}}{\mathrm{Cmax}_{a,j}}\right), & \mathrm{C}_{a,i,t} > \mathrm{Cmax}_{i,j} \end{cases} \tag{S1}$$

where $\mathrm{WP}_{i,t}$ represents the pollution risk of city i on day t. $\mathrm{C}_{a,i,t}$ is the actual concentration level of water quality parameter a of city i on day t. $\mathrm{Cmax}_{a,j}$ indicates the maximum threshold value of the water-using sector j of parameter a.

We perform a related analysis of water scarcity induced by water quality in cities across the country for the national samples we obtain. If $\mathrm{WS}_{\mathrm{quality}}$>1, it indicates that additional withdrawals for water quality deficiencies have exceeded the local availability of water after meeting environmental flow demands. We first calculate the pollution risk of local water quality to the agricultural, industrial, and domestic water sectors through ***Eq. (S1)*** at the city and province level, respectively. Water quality failing to meet standard for each sector during the study period shows consistency at two spatial scales ***(Supplementary Figure 10a, b)***. The risk of water pollution for water use is mainly concentrated in the Songhua, Liaohe, Haihe, Huaihe River basins, the middle and lower reaches of the Yellow River, and the southern Yunnan Province, with frequent industrial and agricultural activities. Linzhi in the Tibet region and Yushu in Qinghai Province show relatively serious risks of pollution (WP>1.5). The southern provinces are generally at low risk of pollution, but occasionally individual cities (e.g., Kunming and Pu'er in Yunnan Province) are relatively polluted (WP>1.5), and local city governments should emphasize water quality issues.

Based on the obtained data on water use sectors in the prefecture-level cities, we further calculate the risk of water scarcity induced by water quality through ***Eqs. (5) and (6)***. The same calculations are made at the provincial level in order to better reflect the national situation and to compensate for urban vacancies in some provinces. From the multi-year situation, both municipal and provincial spatial scales show consistency. Among the prefecture-level cities ***(Supplementary Figure 10c)***, Yuncheng, Liaocheng, Panjin, and Yingkou have $WS_{quality}>1$, and their counterparts in Shanxi Province, Shandong Province, and Liaoning Province have the same $WS_{quality}>1$. These areas are under more severe water stress, with additional withdrawals due to substandard water quality already exceeding the amount of locally available water resources. They have to rely on the exploitation of non-renewable groundwater and inter-basin water transfers such as the South-North Water Transfer Project, and this should also serve as a hotspot for water management matters in the country.

Supplementary Note 2. Study area and summary statistics of main variables

Our study is based on prefecture-level cities, covering most of China's major rivers ***(Supplementary Figure 5a)***. Additionally, the study area is characterized by a distinctive climate ***(Supplementary Figure 5b)***, with an overall trend of higher annual mean temperature in the south and lower in the north.

We conduct summary statistics on our data, including water quality indicators, climate, and economic variables, as shown in ***Supplementary Table 1***. We verify the correlation between the independent variable and the control variable, as shown in ***Supplementary Figure 11***. We also present the regional distribution of water quality indicators as well as yearly time series and capture the frequency of water quality monitoring, as shown in ***Supplementary Figures 6 and 12***. To determine the form of the model's dependent variable, we perform frequency histograms for the three water quality indicators, as shown in ***Supplementary Figure 13***.

Supplementary Note 3. Characteristics of the spatial and temporal distribution of water quality indicators

The spatial distribution of surface water monitoring frequency in China shows a clear east–west gradient, with notable higher monitoring intensity in the eastern and central regions and relatively sparse monitoring in the western and northeastern areas

(Supplementary Figure 12). High-frequency monitoring is concentrated in densely populated and economically developed regions such as the Yangtze River Basin, the Pearl River Delta, the Yangtze River Delta, and the Beijing–Tianjin–Hebei area, reflecting greater water quality pressures and stronger monitoring capacity. In contrast, western and some northeastern regions exhibit lower monitoring intensity, largely due to lower population density, weaker anthropogenic pressures, and higher monitoring costs.

Across the study area, DO concentrations present a geographic pattern, with lower values in southern China and higher values in northern China ***(Supplementary Figure 6a)***. About 6% of the cities in China have DO concentrations below the Class III standard (≤5 mg/L), meaning water quality suitable only for swimming. DO concentrations in the three northeastern provinces are currently at the highest level. A gradual trend of increase in DO concentration is observed with time ***(Supplementary Figure 6b)***. COD_{Mn} concentrations tend to be higher in the northern regions than southern regions, especially in the provinces of Shandong, Hebei, Jilin, and Heilongjiang ***(Supplementary Figure 6c)***. From 2014 to 2015, COD_{Mn} concentrations achieved high levels (>6 mg/L) ***(Supplementary Figure 6d)***, especially in northeastern and central China, failing to meet China's Grade III standard. The highest concentration of NH_3-N is observed in the North China Plain and the three northeastern provinces (i.e., Heilongjiang, Jilin, and Liaoning) ***(Supplementary Figure 6e, f)***. From the overall temporal changes, water pollutants show significant decreasing trends in all regions of China, suggesting the effectiveness of China's water environment treatment since the implementation of the Action Plan for the Prevention and Control of Water Pollution from 2015 onwards.

Supplementary Note 4. Impact of socio-economic variables

River water quality and climate conditions are influenced by human activities. On the one hand, with the advancement of human society, economic growth and production activities in the process of urban development will inevitably have a certain impact on the aquatic environment (Ma et al., 2020). On the other hand, changes in temperature will also have an impact on local economic development (Kotz et al., 2021) and production activities (Hu et al., 2024). Previous studies have confirmed the inverted U-shaped curve of economic development and environmental pollution (Cai et al., 2020; Pandit and Paudel, 2016). Agriculture's nutrient loading is a major source of river pollution (Basu et al., 2022). Industrialization is an important driver of economic growth (Chen et al., 2022), but with high emission characteristics affecting water pollution (Liu and Lin, 2019). Therefore, when fertilizers, wastewater discharges, and pipeline collection change, river pollution alters accordingly (Basu et al., 2022; Cahoon and Hanke, 2019; Vijay et al., 2010).

Supplementary Note 5. Spatial spillover effects of water quality indicators.

Given the high degree of interconnectedness in water ecosystems, water pollution entails significant externalities and spatial spillover effects. To investigate the spatial lag effects of water quality indicators $\sum_{j=1}^{n} \mathrm{Y}_{ij}\mathrm{WQ}_{j,t}$, we employ spatial lag models outlined in ***Eqs. (S2 and S3)***. Here, Y_{ij} denotes the weight between locations i and j, representing the ith and jth component of the spatial weight matrix utilized to account for water quality impacts in neighbouring areas. The spatial weighting matrix is established using inverse distance weighting based on Euclidean distances.

$$\mathrm{lag\_WQ}_{j,t} = \sum_{j=1}^{n} \mathrm{Y}_{ij}\mathrm{WQ}_{j,t} \tag{S2}$$

$$\begin{aligned}\mathrm{lnWQ}_{i,t} = {} & \beta_0 \ln\left(\mathrm{lag\_WQ}_{j,t}\right) + \beta_1 \overline{\mathrm{Temp}}_{i,t} + \beta_2 \overline{\mathrm{Temp}}_{i,t}^2 \\ & + \beta_3 \overline{\mathrm{Temp}}_{i,t} \times \mathrm{Prec}_{i,t} + \eta_1 \mathrm{GDP}_{i,t} + \eta_2 \mathrm{Industry}_{i,t} \\ & + \eta_3 \mathrm{Emission}_{i,t} + \eta_4 \mathrm{Prec}_{i,t} + \alpha_i + \gamma_t + \varepsilon_{i,t}\end{aligned} \tag{S3}$$

Given the highly interconnected water ecosystems, pollutants are transported with flows, yielding spatial spillover effects. We add spatial lag terms for each water quality indicator based on the main model ***(Supplementary Table 2)***. Our results reveal that DO exhibits significant positive spatial spillover effects at different time scales, suggesting that elevated DO levels in neighbouring city rivers are associated with higher DO levels locally. There are no significant spatial spillover effects for COD_{Mn} and NH_3-N. The spatial dependence of DO might arise from similar hydroclimatic conditions ***(Supplementary Figure 5b),*** with similar levels of oxygen solubility in the water bodies and associated biological activities. Alternatively, it is possible that the transfer of other local pollutants (e.g., phosphorus, nitrate-nitrogen) reduces DO in neighboring cities. Furthermore, the spatial lag coefficients of DO decline over short-term scales 1 to 15 days and increase at the monthly scale, indicating that regional climate and activities reinforce spatial correlations over longer periods, which may need further research.

Supplementary Note 6. Heterogeneity analysis of region, river basin and season

To further explore the differences in the impact of air temperature, we select the 15-day scales with the best significant model results ***(Table 2)*** for heterogeneity analysis. We re-assess the main results by partitioning the data into different regional, watershed, and seasonal groups. The distributions of regional and watershed groups are shown in ***Supplementary Figure 8***.

We partition the data into different regional groups according to the geographical distribution and further explore the response of the Northeast, East, West, and Central regions. We define the city group located in Beijing, Tianjin, Shanghai, Hebei, Shandong, Jiangsu, Zhejiang, Fujian, Guangdong Province as the eastern region; located in Heilongjiang, Jilin, Liaoning Province as the northeast region; located in Shanxi, Henan, Hubei, Hunan, Anhui, Jiangxi Province as the central region; located in Chongqing Municipality, Inner Mongolia, Shaanxi, Gansu, Sichuan, Guizhou Province, Ningxia Hui Autonomous Region, Guangxi Zhuang Autonomous Region, Xinjiang Uygur Autonomous Region and Tibet Autonomous Region as the western region. Because river basins have their own heterogeneous characteristics, we also group cities into the Yangtze River Basin and Yellow River Basin sets by their provinces.

In exploring the response of seasonal effects, we define December to February as winter, March to May as spring, June to August as summer, and September to November as autumn, and divided samples based on this. The year-to-year variation of temperature by season is shown in ***Supplementary Figure 9***.

Supplementary Note 7. Robustness tests of main results.

Given the highly distinct seasonal variation in temperature, temperature at seasonal scales may have a significant impact on river water quality. To ensure the robustness of the model results and its broad applicability on time scales, the effect of temperature on water quality is further investigated on seasonal scales and the results are shown in ***Supplementary Table 3*****.**

In temperature studies with daily time scale, daily maximum and minimum temperatures are equally essential variables. To ensure the wide application of the independent variables and to preclude randomness in the data, the average daily temperature data are replaced with the daily maximum, minimum temperatures to observe any changes in ***Eqs. (S4-S5) (Supplementary Table 4)***.

In our third robustness test, acknowledging the seasonal variability of air temperature and its impact on city's water quality, we introduce seasonal fixed effects into our main model to control for seasonal factors, denoted as μ_s in ***Eq. (S6)***, as shown in ***Supplementary Table 5***.

Fourthly, we remove the insignificant interaction term between precipitation and temperature in ***Eq. (1)*** to perform a test on a monthly scale, with the specific setup shown in ***Eq. (S7)***, to ensure the robustness of multiscale models ***(Supplementary Table 6)***.

Finally, we validate our main findings by scaling down the spatial scale of the data to the monitoring sections, ensuring the model's applicability at a smaller spatial scale ***(Supplementary Table 7)***.

$$\begin{aligned} \ln \mathrm{WQ}_{i,t} = {} & \beta_1 \mathrm{Temp}_{\mathrm{Max}_{i,t}} + \beta_2 \mathrm{Temp}_{\mathrm{Max}_{i,t}}^{2} + \beta_3 \mathrm{Temp}_{\mathrm{Max}_{i,t}} \times \mathrm{Prec}_{i,t} \\ & + \eta_1 \mathrm{GDP}_{i,t} + \eta_2 \mathrm{Industry}_{i,t} + \eta_3 \mathrm{Emission}_{i,t} + \eta_4 \mathrm{Prec}_{i,t} \\ & + \alpha_i + \gamma_t + \varepsilon_{i,t} \end{aligned} \tag{S4}$$

$$\begin{aligned} \ln \mathrm{WQ}_{i,t} = {} & \beta_1 \mathrm{Temp}_{\mathrm{Min}_{i,t}} + \beta_2 \mathrm{Temp}_{\mathrm{Min}_{i,t}}^{2} + \beta_3 \mathrm{Temp}_{\mathrm{Min}_{i,t}} \times \mathrm{Prec}_{i,t} \\ & + \eta_1 \mathrm{GDP}_{i,t} + \eta_2 \mathrm{Industry}_{i,t} + \eta_3 \mathrm{Emission}_{i,t} + \eta_4 \mathrm{Prec}_{i,t} \\ & + \alpha_i + \gamma_t + \varepsilon_{i,t} \end{aligned} \tag{S5}$$

$$\begin{aligned} \ln \mathrm{WQ}_{i,t} = {} & \beta_1 \overline{\mathrm{Temp}}_{i,t} + \beta_2 \overline{\mathrm{Temp}}_{i,t}^{2} + \beta_3 \overline{\mathrm{Temp}}_{i,t} \times \mathrm{Prec}_{i,t} + \eta_1 \mathrm{GDP}_{i,t} \\ & + \eta_2 \mathrm{Industry}_{i,t} + \eta_3 \mathrm{Emission}_{i,t} + \eta_4 \mathrm{Prec}_{i,t} + \alpha_i + \gamma_t \\ & + \mu_s + \varepsilon_{i,t} \end{aligned} \tag{S6}$$

$$\begin{aligned} \ln \mathrm{WQ}_{i,t} = {} & \beta_1 \overline{\mathrm{Temp}}_{i,t} + \beta_2 \overline{\mathrm{Temp}}_{i,t}^{2} + \eta_1 \mathrm{GDP}_{i,t} + \eta_2 \mathrm{Industry}_{i,t} \\ & + \eta_3 \mathrm{Emission}_{i,t} + \eta_4 \mathrm{Prec}_{i,t} + \alpha_i + \gamma_t + \varepsilon_{i,t} \end{aligned} \tag{S7}$$

Supplementary Note 8. Selection of Extreme Temperature Model Forms.

We model extreme temperatures with two main types of settings. For the single-day high temperature model, the two specific settings are ***Eqs. (S8-S9)***. For the heatwave, the model specifications are shown in ***Eqs. (S10-S11)***. The results of ***Eqs. (S8-S9)*** are shown in ***Supplementary Tables 8 and 10,*** while ***Eqs. (S10-S11)*** are shown in ***Supplementary Tables 9 and 11***. ***Eqs. (S8 and S10)*** have smaller BICs, while the model is more concise and the results are more consistent and reasonable. Finally, we select

Eqs. (S8) and (S10) as the model forms for the main analysis of extreme temperature analysis and are used in the main text as ***Eqs. (2) and (3)***.

$$\begin{aligned}\ln\mathrm{WQ}_{i,t} = {} & \beta_1\mathrm{Temp}_{\mathrm{Max35}_{i,t}} + \beta_2\mathrm{Temp}_{\mathrm{Max35}_{i,t}}^{2} \\ & + \beta_3\mathrm{Temp}_{\mathrm{Max35}_{i,t}} \times \mathrm{Fertilizer}_{i,t} + \eta_1\mathrm{GDP}_{i,t} \\ & + \eta_2\mathrm{Fertilizer}_{i,t} + \eta_3\mathrm{Agriculture}_{i,t} + \eta_4\mathrm{Industry} \\ & + \eta_5\mathrm{Pipe}_{i,t} + \alpha_i + \gamma_t + \varepsilon_{i,t}\end{aligned} \tag{S8}$$

$$\begin{aligned}\ln\mathrm{WQ}_{i,t} = {} & \beta_1\mathrm{Temp}_{\mathrm{Max35}_{i,t}} + \beta_2\mathrm{Temp}_{\mathrm{Max35}_{i,t}}^{2} \\ & + \beta_3\mathrm{Temp}_{\mathrm{Max35}_{i,t}} \times \mathrm{Fertilizer}_{i,t} \\ & + \beta_4\mathrm{Temp}_{\mathrm{Max35}_{i,t}} \times \mathrm{Prec}_{i,t} + \eta_1\mathrm{GDP}_{i,t} \\ & + \eta_2\mathrm{Fertilizer}_{i,t} + \eta_3\mathrm{Agriculture}_{i,t} \\ & + \eta_4\mathrm{Industry}_{i,t} + \eta_5\mathrm{Pipe}_{i,t} + \eta_6\mathrm{Prec}_{i,t} + \alpha_i + \gamma_t \\ & + \varepsilon_{i,t}\end{aligned} \tag{S9}$$

$$\begin{aligned}\ln\mathrm{WQ}_{i,t} = {} & \beta_1\mathrm{Heatwave}_{i,t} + \eta_1\mathrm{Temp}_{\mathrm{Max35}_{i,t}} + \eta_2\mathrm{Temp}_{\mathrm{Max35}_{i,t}}^{2} \\ & + \eta_3\mathrm{Temp}_{\mathrm{Max35}_{i,t}} \times \mathrm{Fertilizer}_{i,t} + \eta_4\mathrm{GDP}_{i,t} \\ & + \eta_5\mathrm{Fertilizer}_{i,t} + \eta_6\mathrm{Agriculture}_{i,t} \\ & + \eta_7\mathrm{Industry}_{i,t} + \eta_8\mathrm{Pipe}_{i,t} + \alpha_i + \gamma_t + \varepsilon_{i,t}\end{aligned} \tag{S10}$$

$$\begin{aligned}\ln\mathrm{WQ}_{i,t} = {} & \beta_1\mathrm{Heatwave}_{i,t} + \eta_1\mathrm{Temp}_{\mathrm{Max35}_{i,t}} + \eta_2\mathrm{Temp}_{\mathrm{Max35}_{i,t}}^{2} \\ & + \eta_3\mathrm{Temp}_{\mathrm{Max35}_{i,t}} \times \mathrm{Fertilizer}_{i,t} \\ & + \eta_4\mathrm{Temp}_{\mathrm{Max35}_{i,t}} \times \mathrm{Prec}_{i,t} + \eta_5\mathrm{GDP}_{i,t} \\ & + \eta_6\mathrm{Fertilizer}_{i,t} + \eta_7\mathrm{Agriculture}_{i,t} \\ & + \eta_8\mathrm{Industry}_{i,t} + \eta_9\mathrm{Pipe}_{i,t} + \eta_{10}\mathrm{Prec}_{i,t} + \alpha_i \\ & + \gamma_t + \varepsilon_{i,t}\end{aligned} \tag{S11}$$

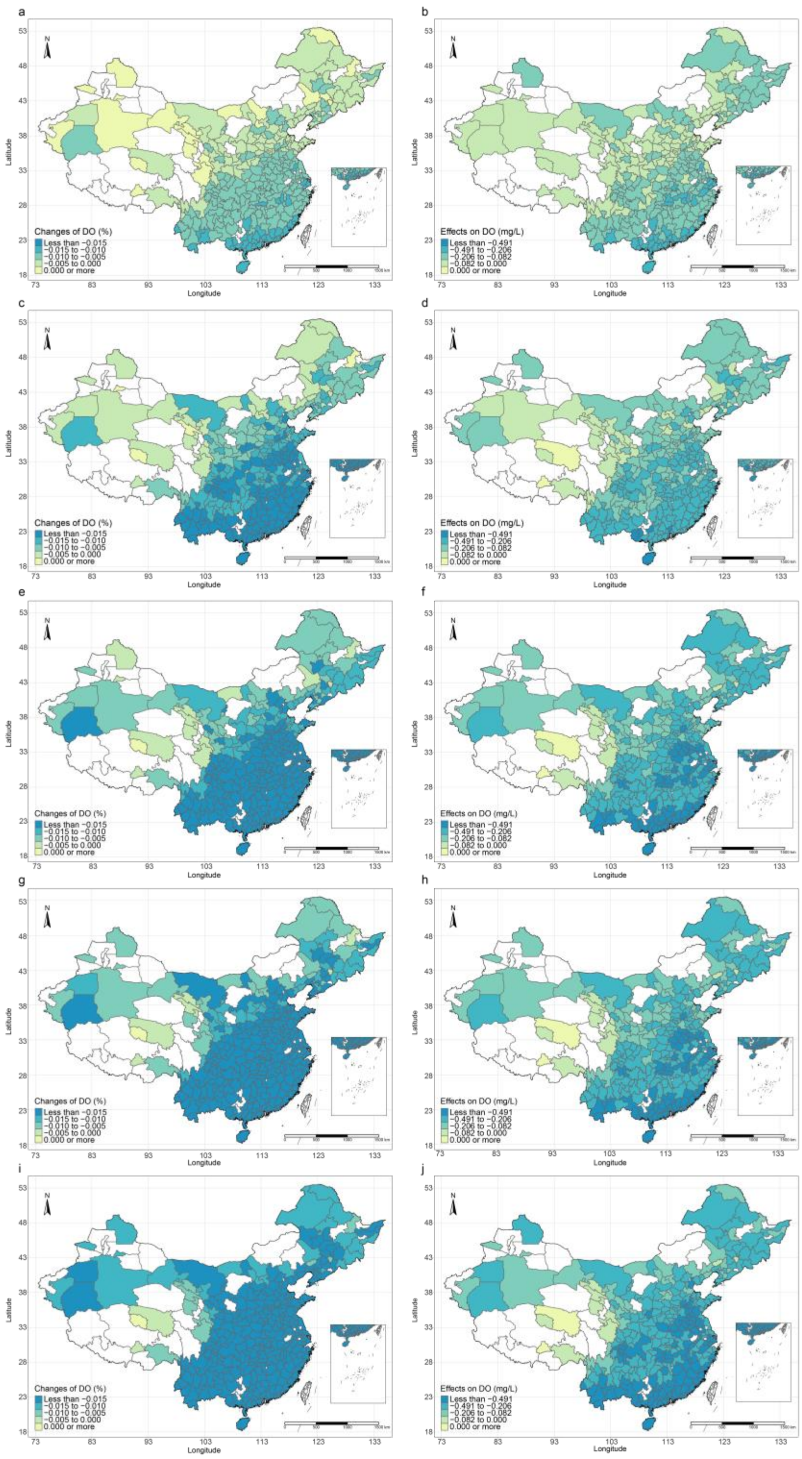

Supplementary Figure 1. Marginal and total effects of temperature on DO at different time scales. (a) Marginal and (b) total effects of temperature on DO at single-day scales. (c) Marginal and (d) total effects of temperature on DO at five-day scales. (e) Marginal and (f) total effects of temperature on DO at ten-day scales. (g) Marginal and (h) total effects of temperature on DO at fifteen-day scales. (i) Marginal and (j) total effects of temperature on DO at monthly scales.

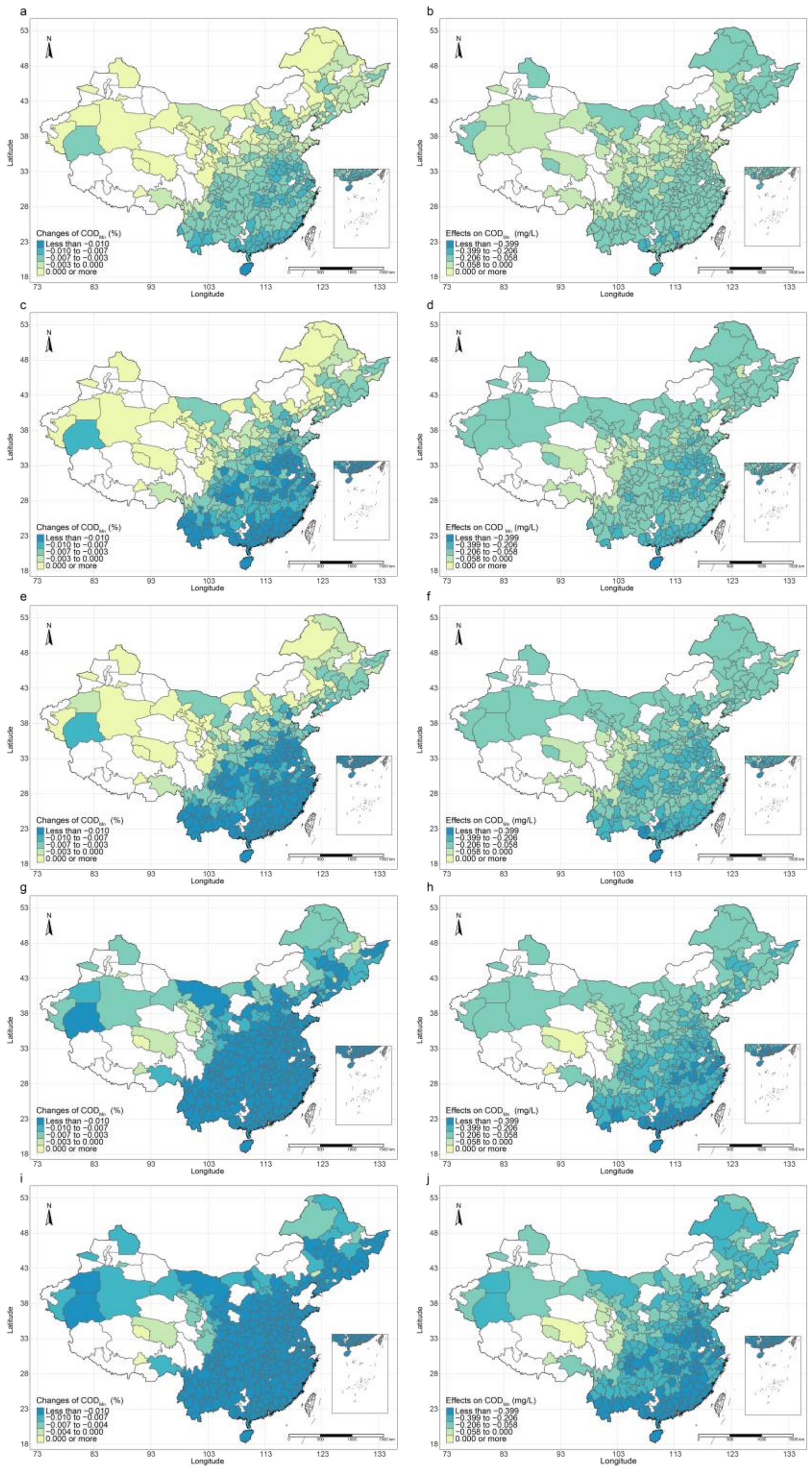

Supplementary Figure 2. Marginal and total effects of temperature on COD$_{Mn}$ at different time scales. (a) Marginal and (b) total effects of temperature on COD$_{Mn}$ at single-day scales. (c) Marginal and (d) total effects of temperature on COD$_{Mn}$ at five-day scales. (e) Marginal and (f) total effects of temperature on COD$_{Mn}$ at ten-day scales. (g) Marginal and (h) total effects of temperature on COD$_{Mn}$ at fifteen-day scales. (i) Marginal and (j) total effects of temperature on COD$_{Mn}$ at monthly scales.

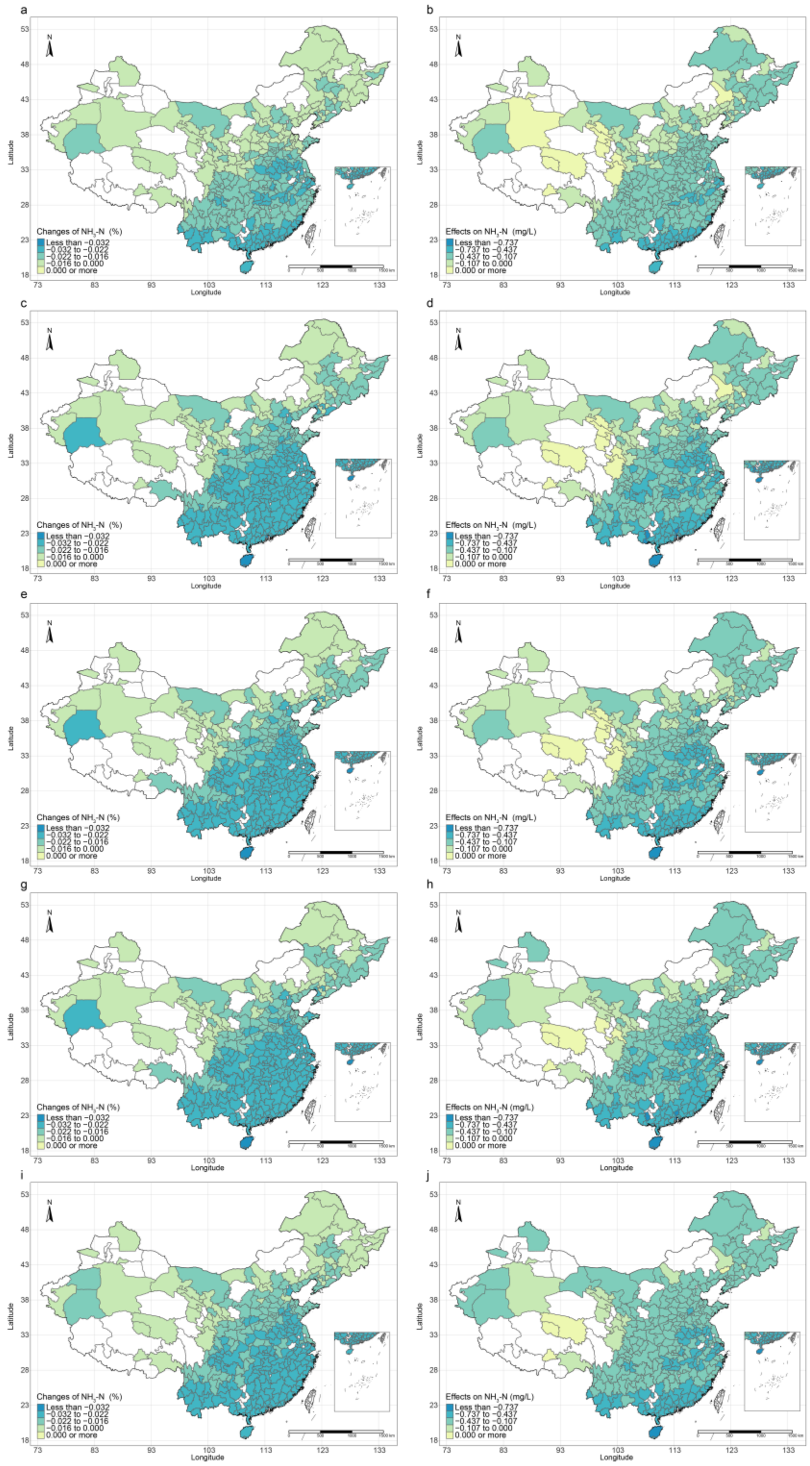

Supplementary Figure 3. Marginal and total effects of temperature on NH_3-N at different time scales. (a) Marginal and (b) total effects of temperature on NH_3-N at single-day scales. (c) Marginal and (d) total effects of temperature on NH_3-N at five-day scales. (e) Marginal and (f) total effects of temperature on NH_3-N at ten-day scales. (g) Marginal and (h) total effects of temperature on NH_3-N at fifteen-day scales. (i) Marginal and (j) total effects of temperature on NH_3-N at monthly scales.

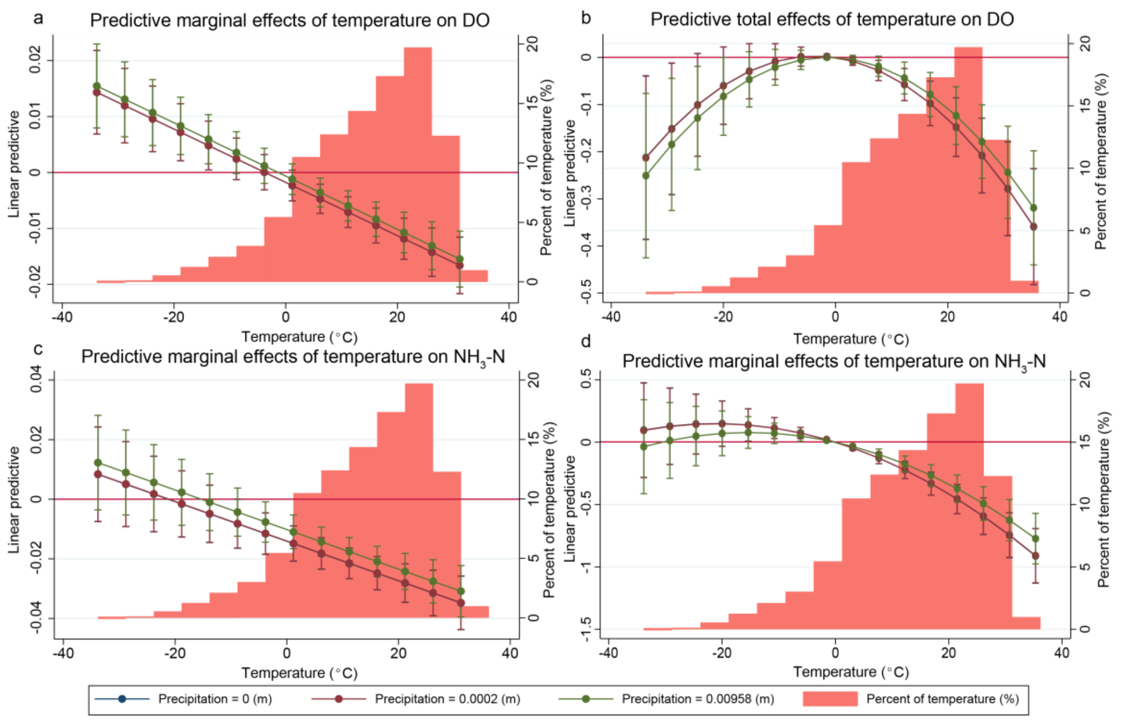

Supplementary Figure 4. Marginal and total effects of temperature on DO and NH_3-N at different precipitation levels. (a) Marginal effects of temperature on DO. (b) Total effects of temperature on DO. (c) Marginal effects of temperature on NH_3-N. (d) Total effects of temperature on NH_3-N.

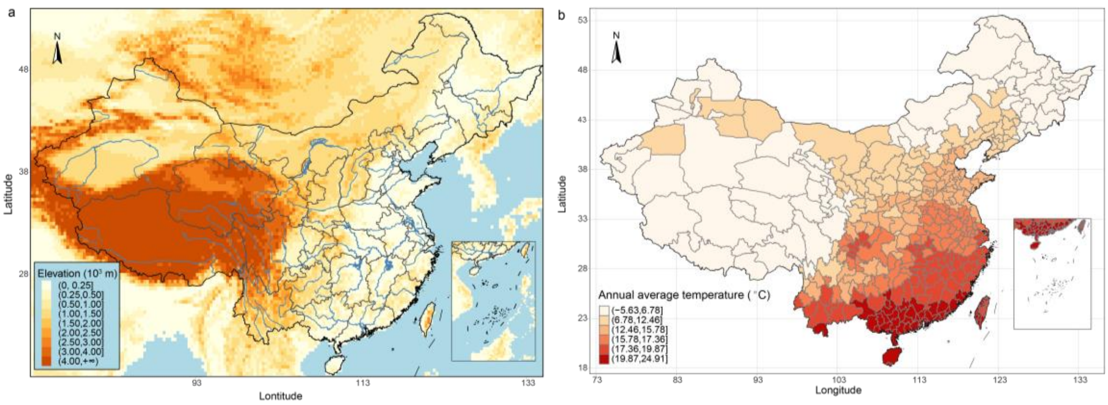

Supplementary Figure 5. Spatial distribution of river basins and temperature in China. (a) Spatial distribution of rivers. (b) Annual average of temperature for the period 2014-2020.

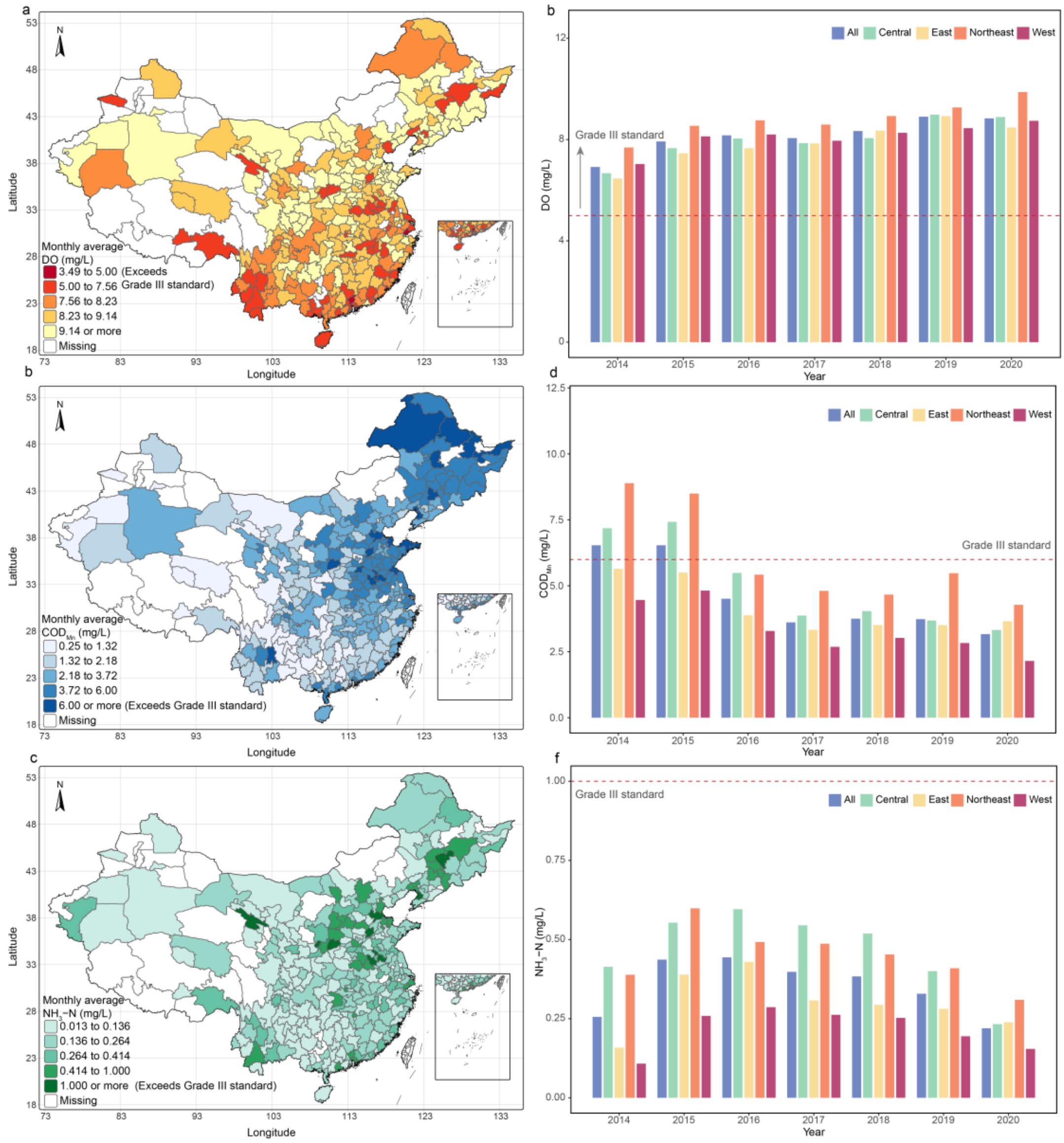

Supplementary Figure 6. The spatial and temporal distribution of monthly average of water quality indicators. (a) Spatial and **(b)** temporal distribution of the monthly average DO. **(c)** Spatial and **(d)** temporal distribution of monthly average COD_{Mn}. **(e)** Spatial and **(f)** temporal distribution of monthly average NH_3-N.

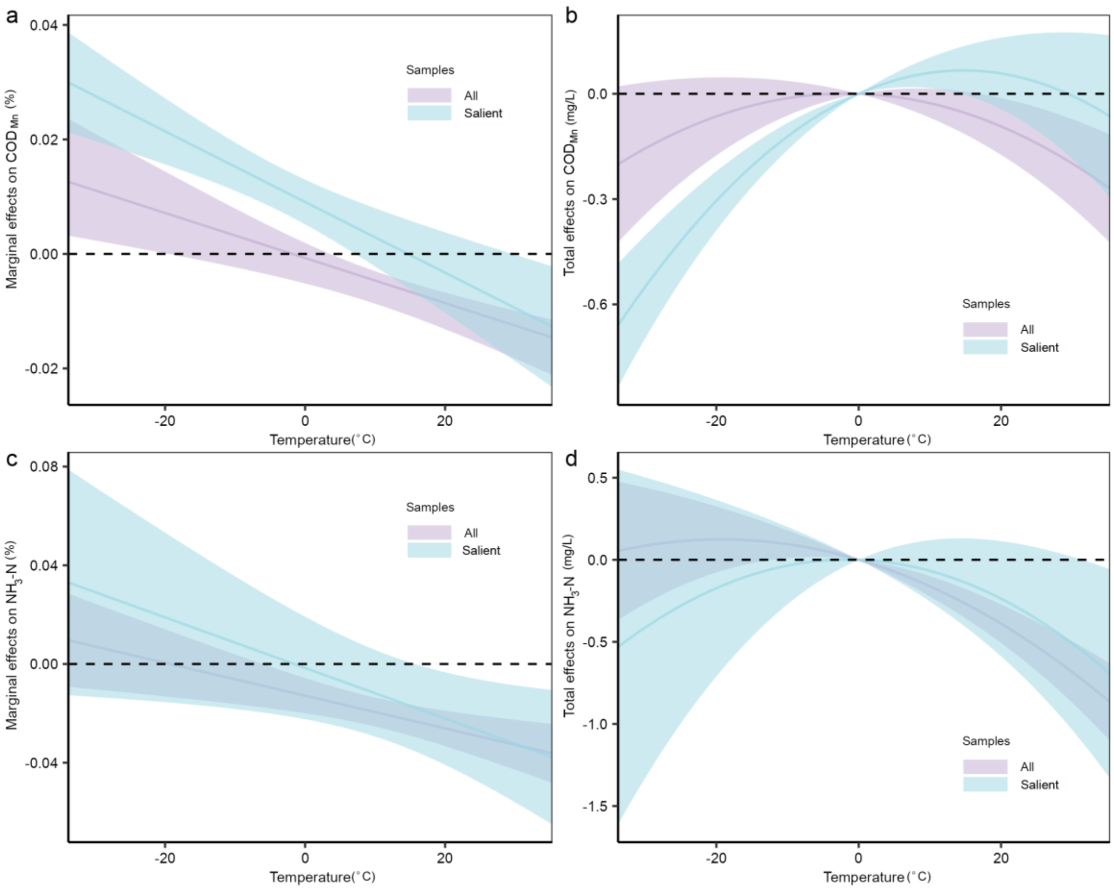

Supplementary Figure 7. Marginal and total effects of temperature on COD_{Mn} and NH_3-N in Hai River as well as the middle and lower reaches of the Yellow River which has high water quality baselines (salient samples). (a) Marginal effects of temperature on COD_{Mn}. (b) Total effects of temperature on COD_{Mn}. (c) Marginal effects of temperature on NH_3-N. (d) Total effect of temperature on NH_3-N.

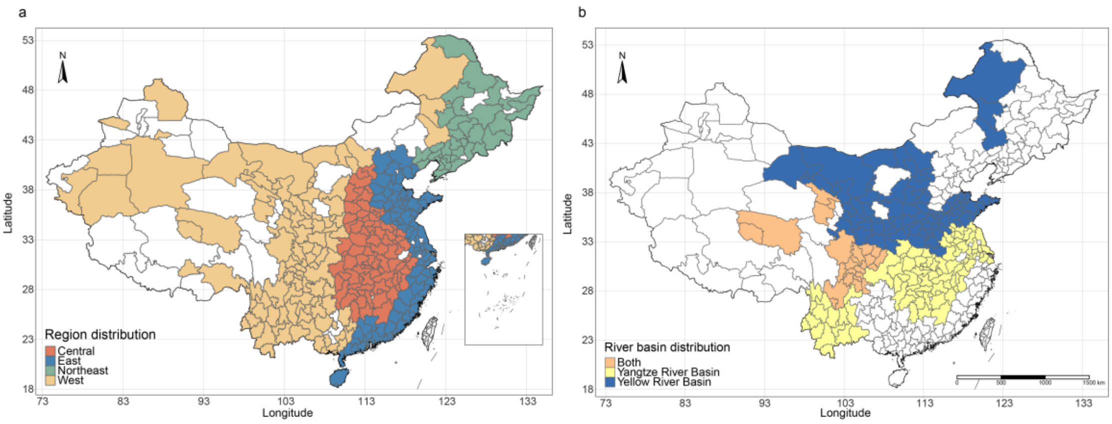

Supplementary Figure 8. Division of region and river basin. (a) Distribution of the cities by geographic location. (b) Location of the cities in the basin according to province.

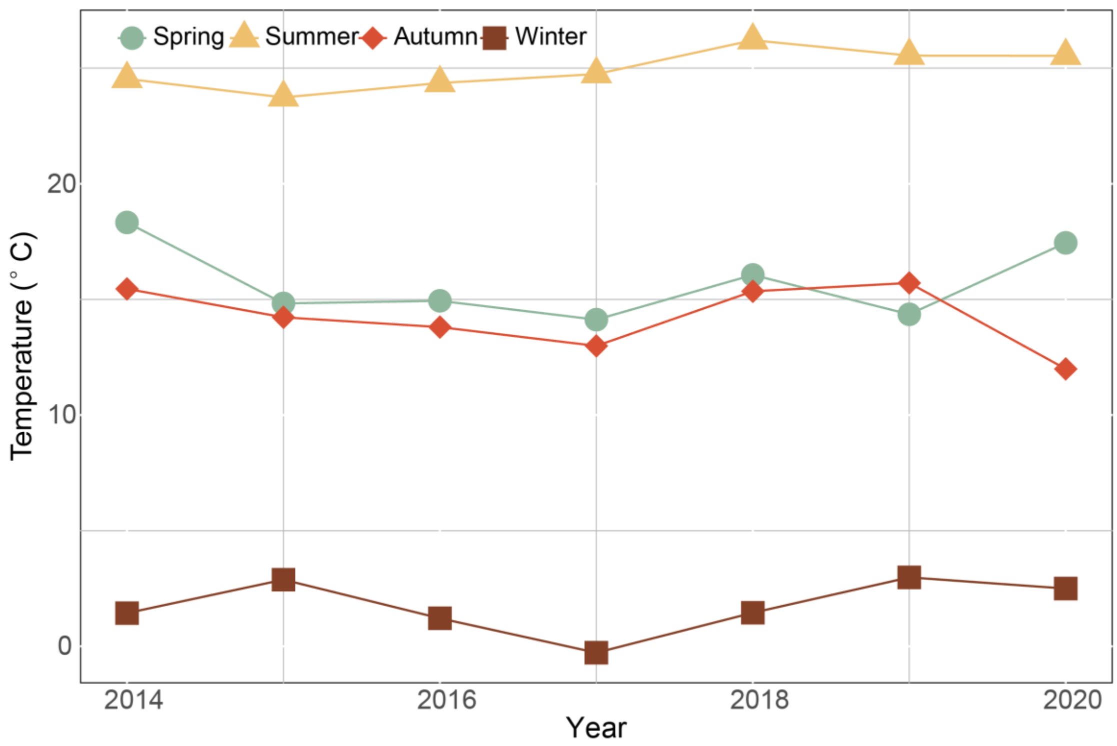

Supplementary Figure 9. Time series of seasonal average temperature of different seasons in China from 2014 to 2020.

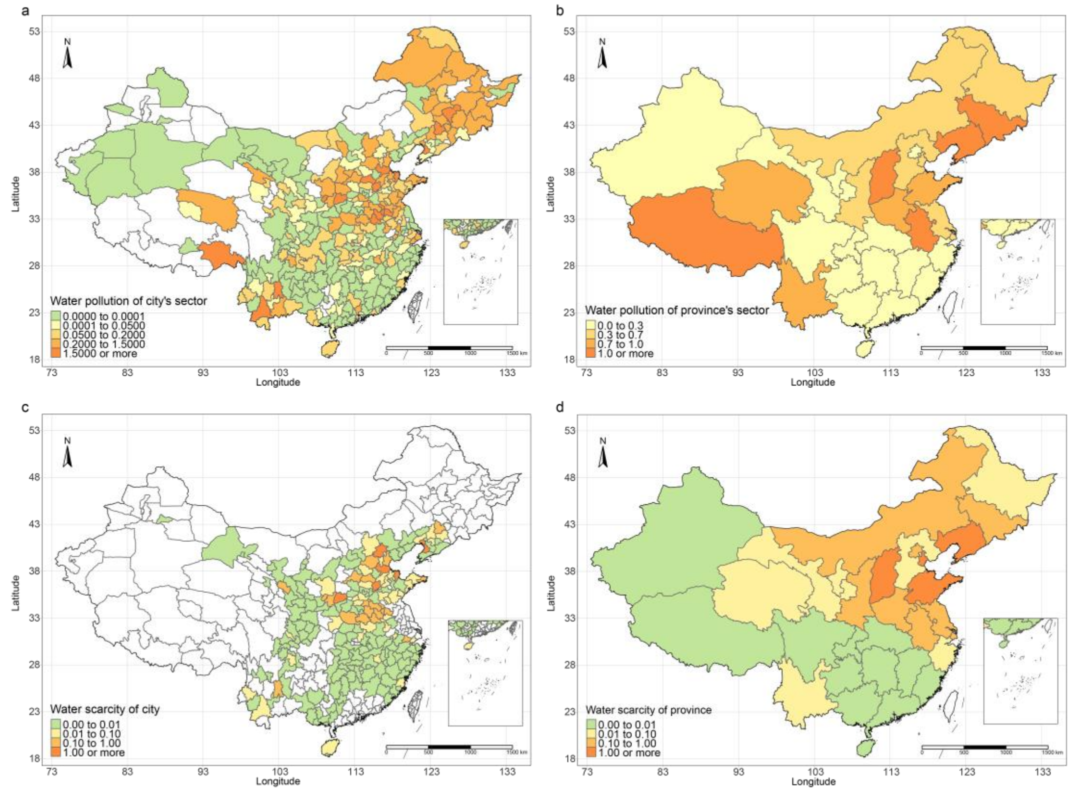

Supplementary Figure 10. Risk of water pollution and water scarcity induced by water quality in the water-using sectors of cities and provinces in the country. (a) Risk of water pollution in the urban water use sector in the country. (b) Risk of water pollution in the provincial water sector. (c) Risk of water scarcity induced by water quality in the urban water sector. (d) Risk of water scarcity induced by water quality in the provincial water sector.

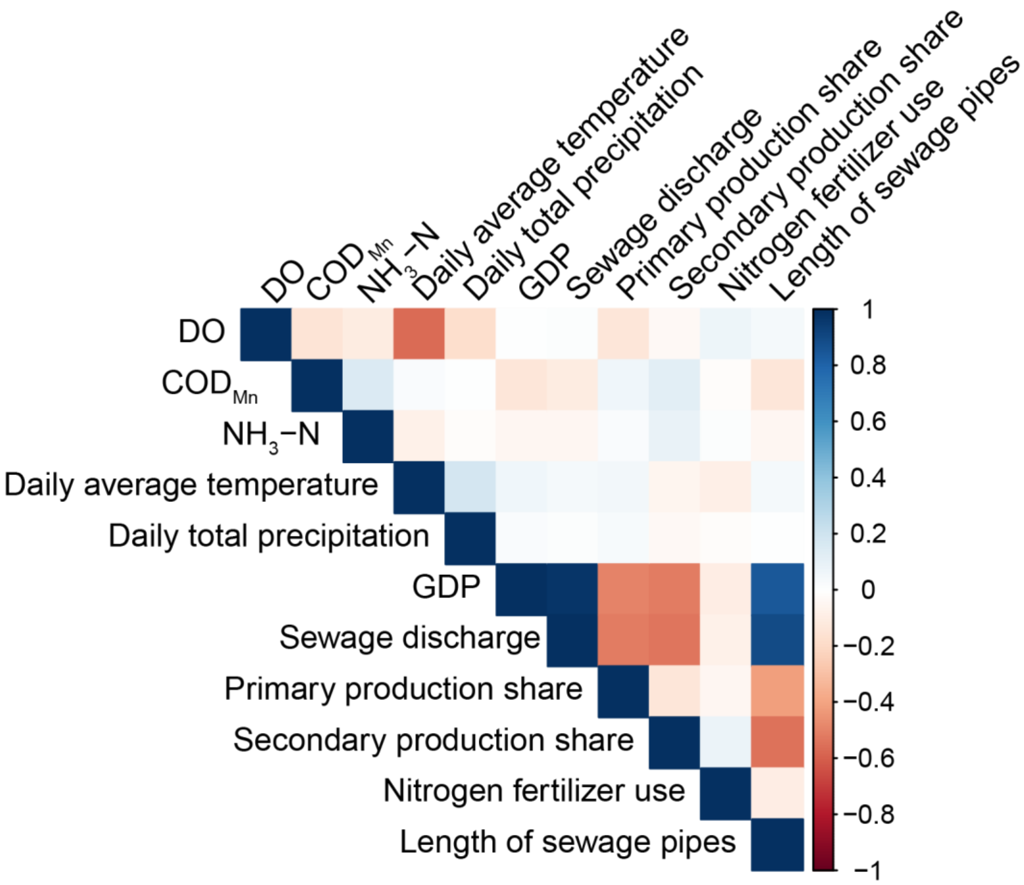

Supplementary Figure 11. Correlation heatmap of variables.

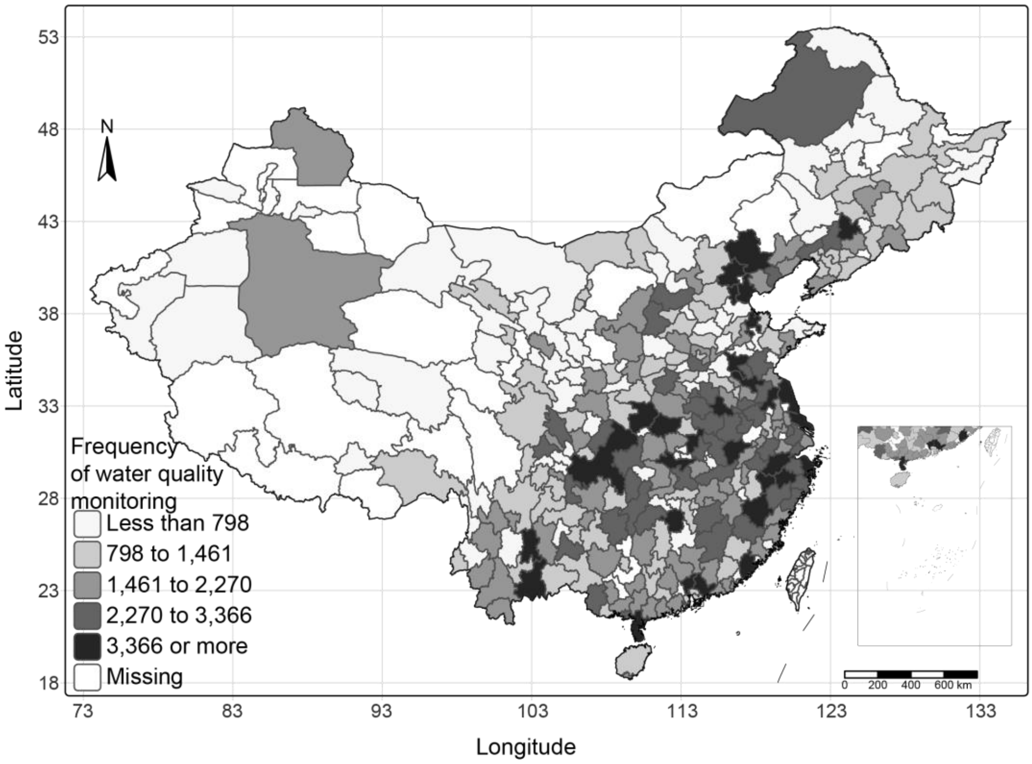

Supplementary Figure 12. Regional distribution of the annual frequency of water quality monitoring.

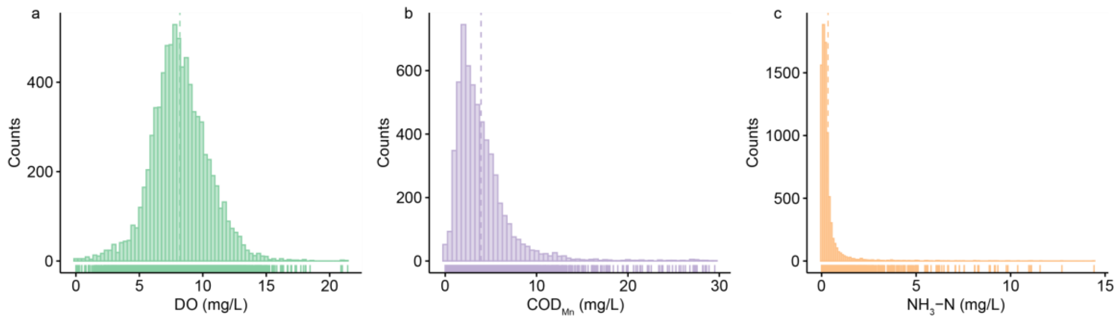

Supplementary Figure 13. Concentration and frequency distribution of water quality indicators, including (a) DO, (b) COD_{Mn}, and (c) NH_3-N.

Supplementary Table 1. Descriptive statistics of the dataset used for the analysis.

Variables	Mean	SD	Median	Min	Max	Unit
Daily DO	8.18	2.46	8.00	0.01	24.44	mg/L
Daily COD_{Mn}	3.94	3.06	3.22	0.01	29.95	mg/L
Daily NH_3-N	0.42	0.93	0.20	0.001	19.82	mg/L
Daily average temperature	14.31	11.14	16.26	-33.82	35.32	℃
Daily total precipitation	0.003	0.01	0.00	0.00	0.21	m
GDP	403.06	569.53	204.518	9.286	3870.06	10^8CNY
Sewage discharge	2.21	3.76	0.80	0.10	23.62	$10^8 m^3$
Percentage of primary production	0.11	0.08	0.41	0.00	0.50	%
Percentage of secondary production	0.43	0.10	0.42	0.08	0.69	%
Nitrogen fertilizer use	9.31	9.10	7.20	0.18	49.9	10^4 tons
Length of sewage pipes	1215.41	2151.69	430.76	5.00	26323.91	km

Supplementary Table 2. Panel regression results for the spatial spillover models.

	(1) DO 1 Day	(2) COD_{Mn} 1 Day	(3) NH_3-N 1 Day	(4) DO 5 Day	(5) COD_{Mn} 5 Day	(6) NH_3-N 5 Day
Temp	-0.00218	-0.000632	-0.0138***	-0.00563***	-0.0046*	-0.0162***
	(0.0017)	(0.0023)	(0.0038)	(0.0018)	(0.0028)	(0.0047)
Temp^2	-0.000197***	-0.000198***	-0.000308***	-0.000342***	-0.000293***	-0.000409***
	(0.000057)	(0.00005)	(0.00011)	(0.000064)	(0.000056)	(0.00014)
GDP	-0.000141*	0.000105	0.000364	-0.000146*	0.000126	0.00048
	(0.000073)	(0.00034)	(0.00057)	(0.000075)	(0.00037)	(0.00067)
Industry	0.3	0.731	-0.0991	0.325	0.71	-0.268
	(0.23)	(0.77)	(0.72)	(0.23)	(0.85)	(0.81)
Emission	0.0257	-0.0569	-0.0728	0.0281	-0.043	-0.0845
	(0.018)	(0.061)	(0.13)	(0.019)	(0.066)	(0.14)
Lag DO	0.00123***			0.000979***		
	(0.00033)			(0.00034)		
Lag COD_{Mn}		-0.00275			-0.00286	
		(0.0018)			(0.0019)	
Lag NH_3*-N*			0.0124			0.00929
			(0.011)			(0.014)
Prep	-3.93***	-1.58	-8.63***	-2***	-0.169	-1.2
	(1.1)	(1.8)	(2.8)	(0.61)	(0.98)	(1.6)
Temp × *Prep*	0.11**	0.0546	0.391***	0.052*	0.0163	0.0989
	(0.052)	(0.078)	(0.13)	(0.028)	(0.044)	(0.069)
N	170752	118489	135182	36243	25557	29846
adj. R^2	0.439	0.594	0.475	0.466	0.602	0.461
BIC	53708	141627	314248	6370	30475	69079

Note: The coefficients are the regression results of the main models for DO, COD_{Mn}, and NH_3-N, representing the 100%-point effect on water quality per unit increase for a given temperature. '*Temp*', the average air temperature; '*Prec*', total precipitation; '*GDP*', total GDP; '*Industry*', the percentage of GDP output of the secondary sector; '*Emission*', wastewater discharged; '*LagDO*', '*LagCOD*$_{Mn}$', and '*LagNH*$_3$*-N*' represent the logarithm of the spatial lag term for DO, COD_{Mn}, and NH_3-N, respectively. '*N*', the number of observations. Standard errors are clustered at the municipal level and are shown in parenthesis. (* $p < 0.1$, ** $p < 0.05$, *** $p < 0.01$.)

Supplementary Table 2. Continued.

	(7) DO 10 Day	(8) COD_{Mn} 10 Day	(9) NH_3-N 10 Day	(10) DO 15 Day	(11) COD_{Mn} 15 Day	(12) NH_3-N 15 Day
Temp	-0.00774***	-0.00759**	-0.0168***	-0.00923***	-0.0093***	-0.00165***
	(0.0019)	(0.003)	(0.0055)	(0.0019)	(0.0032)	(0.006)
$Temp^2$	-0.000448***	-0.000353***	-0.000493***	-0.000517***	-0.000418***	-0.000536***
	(0.000068)	(0.000062)	(0.00017)	(0.00007)	(0.000077)	(0.00019)
GDP	-0.000143*	0.000169	0.000541	-0.000139*	0.000165	0.000583
	(0.000077)	(0.00037)	(0.00076)	(0.000077)	(0.00038)	(0.00078)
Industry	0.275	0.64	-0.401	0.259	0.663	-0.475
	(0.22)	(0.83)	(0.89)	(0.23)	(0.85)	(0.92)
Emission	0.0303	-0.0334	-0.0843	0.0304	-0.0377	-0.0851
	(0.021)	(0.069)	(0.15)	(0.02)	(0.065)	(0.15)
Lag DO	0.000702**			0.000542*		
	(0.00033)			(0.00033)		
Lag COD_{Mn}		-0.00236			-0.00191	
		(0.0019)			(0.002)	
Lag NH_3-N			0.00382			0.00667
			(0.016)			(0.018)
Prep	-1.39***	0.574	-1.01	-1.25***	0.268	-0.0794
	(0.45)	(0.7)	(1.3)	(0.38)	(0.78)	(1.2)
Temp × *Prep*	0.0345*	-0.0189	0.0769	0.0337**	-0.00475	0.0384
	(0.02)	(0.032)	(0.057)	(0.016)	(0.033)	(0.05)
N	18790	13448	15860	12866	9312	11108
adj. R^2	0.476	0.606	0.461	0.475	0.603	0.471
BIC	2208	15818	36905	1416	11006	26208

Note: The coefficients are the regression results of the main models for DO, COD_{Mn}, and NH_3-N, representing the 100%-point effect on water quality per unit increase for a given temperature. '*Temp*', the average air temperature; '*Prec*', total precipitation; '*GDP*', total GDP; '*Industry*', the percentage of GDP output of the secondary sector; '*Emission*', wastewater discharged; '*LagDO*', '*LagCOD$_{Mn}$*' and '*LagNH$_3$-N*' represent the logarithm of the spatial lag term for DO, COD_{Mn} and NH_3-N, respectively. '*N*', the number of observations. Standard errors are clustered at the municipal level and are shown in parenthesis. (* $p < 0.1$, ** $p < 0.05$, *** $p < 0.01$.)

Supplementary Table 2. Continued.

	(13) DO Month	(14) COD_{Mn} Month	(15) NH_3-N Month
Temp	-0.0112***	-0.0000278	0.0156
	(0.0034)	(0.01)	(0.015)
$Temp^2$	-0.000586***	-0.000503*	0.0000223
	(0.00012)	(0.00026)	(0.00045)
GDP	-0.0000606	-0.0048	0.00618**
	(0.00059)	(0.007)	(0.003)
Industry	1.09	0.995	-14.2**
	(0.82)	(4.5)	(5.9)
Emission	-0.265**	0.18	0.977***
	(0.11)	(0.15)	(0.26)
Lag	0.00154*		
DO	(0.00081)		
Lag		-0.000497	
COD_{Mn}		(0.0016)	
Lag			0.0523
NH_3-*N*			(0.047)
Prep	-1.62***	-0.58	2.82
	(0.56)	(2)	(2.6)
Temp × *Prep*	0.0638***	0.0439	-0.0283
	(0.024)	(0.081)	(0.11)
N	1849	1156	1313
adj. R^2	0.601	0.765	0.616
BIC	322	1106	3260

Note: The coefficients are the regression results of the main models for DO, COD_{Mn}, and NH_3-N, representing the 100%-point effect on water quality per unit increase for a given temperature. '*Temp*', the average air temperature; '*Prec*', total precipitation; '*GDP*', total GDP; '*Industry*', the percentage of GDP output of the secondary sector; '*Emission*', wastewater discharged; '*LagDO*', '$LagCOD_{Mn}$' and '$LagNH_3$-*N*' represent the logarithm of the spatial lag term for DO, COD_{Mn} and NH_3-N, respectively. '*N*', the number of observations. Standard errors are clustered at the municipal level and are shown in parenthesis. (* $p < 0.1$, ** $p < 0.05$, *** $p < 0.01$.)

263 **Supplementary Table 3. Robustness test results for extending the time scale to the**
264 **seasonal scale.**

	(1) DO	(2) COD_{Mn}	(3) NH_3-N
Temp	-0.0112***	-0.012**	-0.00736
	(0.0021)	(0.0049)	(0.0094)
$Temp^2$	-0.000699***	-0.000339***	-0.00039
	(0.000084)	(0.00013)	(0.00027)
Prec	-0.256**	0.31	0.264
	(0.12)	(0.19)	(0.43)
GDP	-0.000139*	0.000349	0.000574
	(0.000081)	(0.00035)	(0.00089)
Industry	0.142	0.266	-0.347
	(0.21)	(0.69)	(1.1)
Emission	0.0419	-0.024	-0.0925
	(0.026)	(0.046)	(0.14)
Temp×Prec	0.00923	-0.0133	-0.000893
	(0.0066)	(0.0083)	(0.019)
N	2804	2219	2679
adj. R^2	0.553	0.668	0.538
BIC	-1262	1792	6114

Note: The coefficients are the regression results of the main models for DO, COD_{Mn}, and NH_3-N, representing the 100%-point effect on water quality per unit increase for a given temperature. 'Temp', the average air temperature; 'Prec', total precipitation; 'GDP', total GDP; 'Industry', the percentage of GDP output of the secondary sector; 'Emission', wastewater discharged; 'N', the number of observations. Standard errors are clustered at the municipal level and are shown in parenthesis. (* $p < 0.1$, ** $p < 0.05$, *** $p < 0.01$.)

265

Supplementary Table 4. Robustness test results of replacing the dependent variable with daily maximum temperature and the daily minimum temperature.

	(1) DO	(2) COD_{Mn}	(3) NH_3-N	(4) DO	(5) COD_{Mn}	(6) NH_3-N
$Temp_{Max}$	0.00067 (0.0025)	0.00149 (0.0024)	-0.00913 (0.0057)			
$Temp_{Max}^2$	-0.000116* (0.000059)	-0.000146** (0.000057)	-0.000262** (0.00013)			
$Temp_{Min}$				-0.00689*** (0.0018)	-0.00496** (0.0022)	-.0181*** (.0041)
$Temp_{Min}^2$				-0.000253*** (0.000053)	-0.000181*** (0.00006)	-.000282** (.00012)
Prec	-4.57*** (1.3)	-1.27 (1.8)	-11*** (3.3)	-3.19*** (1)	0.422 (1.5)	-5.11** (2.4)
GDP	-0.000167** (0.000079)	0.000242 (0.00033)	0.000568 (0.00062)	-0.000166** (0.00008)	0.000235 (0.00033)	.000565 (.00062)
Industry	0.488 (0.3)	-0.668 (0.67)	-0.963 (0.96)	0.486 (0.31)	-0.664 (0.67)	-.955 (0.96)
Emission	0.0241 (0.018)	-0.055 (0.063)	-0.0715 (0.13)	0.0239 (0.018)	-0.0544 (0.063)	-0.0716 (0.13)
$Temp_{Max}$× Prec	0.132** (0.053)	0.0342 (0.07)	0.426*** (0.13)			
$Temp_{Min}$× Prec				0.101* (0.054)	-0.0241 (0.07)	0.328*** (0.12)
N	153888	107501	122285	153888	107501	122285
adj. R^2	0.438	0.596	0.481	0.444	0.596	0.481
BIC	54792	123964	285318	53343	123828	285360

Note: The coefficients are the regression results of the main models for DO, COD_{Mn}, and NH_3-N, representing the 100%-point effect on water quality per unit increase for a given temperature. '$Temp_{max}$', the daily maximum air temperature; '$Temp_{min}$', the daily minimum air temperature; 'Prec', total daily precipitation; 'GDP', total GDP; 'Industry', the percentage of GDP output of the secondary sector; 'Emission', wastewater discharged; 'N', the number of observations. Standard errors are clustered at the municipal level and are shown in parenthesis. (* $p < 0.1$, ** $p < 0.05$, *** $p < 0.01$.)

Supplementary Table 5. Robustness test results for adding seasonal fixed effects to the fixed effects term.

	(1) DO	(2) COD_{Mn}	(3) NH_3-N
Temp	-0.0025	-0.00182	-0.0153***
	(.0021)	(0.0023)	(0.0047)
$Temp^2$	-0.000201***	-0.000179***	-0.000339**
	(0.000059)	(0.000061)	(0.00013)
Prec	-3.24***	-0.0191	-7.97***
	(1.1)	(1.5)	(2.6)
GDP	-0.000166**	0.000238	0.000567
	(0.00008)	(0.00033)	(0.00062)
Industry	0.487	-0.667	-0.966
	(0.3)	(0.67)	(0.96)
Emission	0.0239	-0.0546	-0.0717
	(0.018)	(0.063)	(0.13)
Temp×Prec	0.0817	-0.0237	0.393***
	(0.056)	(0.071)	(0.13)
N	153888	107501	122285
adj. R^2	0.441	0.596	0.481
BIC	54127	123876	285188

Note: The coefficients are the regression results of the main models for DO, COD_{Mn}, and NH_3-N, representing the 100%-point effect on water quality per unit increase for a given temperature. 'Temp' the daily air temperature; 'Prec' total daily precipitation; 'GDP', total GDP; 'Industry', the percentage of GDP output of the secondary sector; 'Emission', wastewater discharged; 'N', the number of observations. Standard errors are clustered at the municipal level and are shown in parenthesis. (* $p < 0.1$, ** $p < 0.05$, *** $p < 0.01$.)

Supplementary Table 6. Robustness test results of removing the interaction term between precipitation and temperature on the month scale.

	(1) DO	(2) COD_{Mn}	(3) NH_3-N
Temp	-0.0109***	-0.0107***	-0.0139**
	(0.002)	(0.0039)	(0.0067)
$Temp^2$	-0.000575***	-0.000487***	-0.000498***
	(0.000059)	(0.000093)	(0.00018)
Prec	-0.222***	0.137	0.598***
	(0.059)	(0.13)	(0.2)
GDP	-0.000132*	0.000249	0.000687
	(0.000077)	(0.0004)	(0.00084)
Industry	0.229	0.426	-0.599
	(0.22)	(0.84)	(1)
Emission	0.0329	-0.0423	-0.096
	(0.022)	(0.066)	(0.16)
N	6803	5037	6123
adj. R^2	0.482	0.607	0.495
BIC	403	5673	14679

Note: The coefficients are the regression results of the main models for DO, COD_{Mn}, and NH_3-N, representing the 100%-point effect on water quality per unit increase for a given temperature. 'Temp', the monthly average air temperature; 'Prec', total monthly precipitation; 'GDP', total GDP; 'Industry', the percentage of GDP output of the secondary sector; 'Emission', wastewater discharged; 'N', the number of observations. Standard errors are clustered at the municipal level and are shown in parenthesis. (* $p < 0.1$, ** $p < 0.05$, *** $p < 0.01$.)

Supplementary Table 7. Results of a robustness check when spatial scales are at monitoring sections.

	(1) DO	(2) COD_{Mn}	(3) NH_3-N
Temp	-0.0105***	0.0000178	-0.0133**
	(0.0018)	(0.0029)	(0.0058)
$Temp^2$	-0.000492***	-0.00052***	-0.00012
	(0.000076)	(0.00011)	(0.0002)
Prec	-0.577**	-0.0679	1.11
	(0.25)	(0.52)	(0.81)
GDP	0.000115	-0.00138**	0.00105
	(0.00014)	(0.00063)	(0.00075)
Industry	0.161	0.664	-1.63
	(0.22)	(0.72)	(1.2)
Emission	-0.0144	0.111*	-0.0768
	(0.022)	(0.064)	(0.1)
Temp×Prec	0.0167	0.00777	-0.0276
	(0.011)	(0.022)	(0.034)
N	9658	8412	8970
adj. R^2	0.532	0.761	0.640
BIC	-4556	4790	19492

Note: The coefficients are the regression results of the main models for DO, COD_{Mn}, and NH_3-N, representing the 100%-point effect on water quality per unit increase for a given temperature. '*Temp*', the average air temperature; '*Prec*', total precipitation; '*GDP*', total GDP; '*Industry*', the percentage of GDP output of the secondary sector; '*Emission*', wastewater discharged; '*N*', the number of observations. Standard errors are clustered at the station level and are shown in parenthesis. (* $p < 0.1$, ** $p < 0.05$, *** $p < 0.01$.)

Supplementary Table 8. Impacts of single-day high temperatures.

	(1) DO	(2) COD_{Mn}	(3) NH_3-N	(4) DO	(5) COD_{Mn}	(6) NH_3-N
$Temp_{Max35}$	-0.00521	-0.00557	-0.02	-0.878	-3^{*}	-2.26
	(0.0043)	(0.0047)	(0.012)	(1.8)	(1.7)	(2.1)
$Temp_{Max35}^2$	0.0000132	0.0000577	-0.0000729	0.0132	0.041^{*}	0.0295
	(0.000093)	(0.00014)	(0.00023)	(0.025)	(0.022)	(0.029)
fert	-0.00144	-0.0343^{***}	0.00151	0.125	-0.161	-0.127
	(0.0027)	(0.006)	(0.0083)	(0.1)	(0.13)	(0.28)
GDP	-0.0301^{*}	0.041	0.125^{*}	-0.0432	0.196^{***}	0.374^{*}
	(0.018)	(0.068)	(0.064)	(0.061)	(0.059)	(0.2)
$Temp_{Max35} \times fert$	0.000193	-0.000196	0.000139	-0.00384	0.00169	0.00401
	(0.00012)	(0.00026)	(0.00046)	(0.0028)	(0.0034)	(0.0062)
Industry	0.071	0.983	0.692	-0.965	0.612	-4.65
	(0.72)	(1.3)	(2)	(1.5)	(1.6)	(4.3)
Agriculture	-2.16	1.39	4.56	-1.22	0.835	-0.375
	(1.6)	(1.9)	(3.4)	(2.8)	(2.6)	(5)
Pipe	-0.000046	-0.0000908	0.0000795	0.0000155	0.000387	0.000597^{**}
	(0.000037)	(0.00011)	(0.00011)	(0.00014)	(0.00036)	(0.00029)
N	60703	46239	48541	1140	876	991
adj. R^2	0.429	0.567	0.476	0.410	0.428	0.481
BIC	34736	53091	113560	1021	597	2125

Note: The coefficients are the regression results of the single-day high temperature models for DO, COD_{Mn}, and NH_3-N, representing the 100%-point effect on water quality per unit increase for a given temperature. '$Temp_{Max35}$' the daily maximum air temperature; '*fert*', nitrogen application rate; '*GDP*', total GDP; '*Secondary*', the percentage of GDP output of the secondary sector; '*Primary*', the percentage of GDP output of the primary sector; '*Pipe*', length of drainage pipe; '*N*', the number of observations. Standard errors are clustered at the municipal level and are shown in parenthesis. ($^{*}p < 0.1$, $^{**}p < 0.05$, $^{***}p < 0.01$.)

Columns 1-3 show the regression results for the samples with daily maximum temperature below 35℃, and ***columns 4-6*** show the results for the samples with daily maximum temperature above 35℃.

Supplementary Table 9. Results of the impacts for heatwave.

	(1) DO	(2) COD_{Mn}	(3) NH_3-N	(4) DO	(5) COD_{Mn}	(6) NH_3-N
twodays	-0.0322	0.0863**	0.00306			
	(0.051)	(0.041)	(0.1)			
threedays				-0.0721	0.0591	0.0535
				(0.052)	(0.042)	(0.12)
fourdays						
$Temp_{Max35}$	-0.694	-3.54**	-2.28	-0.771	-3.1*	-2.36
	(1.9)	(1.7)	(2.2)	(1.8)	(1.6)	(2.1)
$Temp_{Max35}^2$	0.0108	0.0481**	0.0297	0.0119	0.0422*	0.0307
	(0.026)	(0.023)	(0.03)	(0.024)	(0.022)	(0.028)
fert	0.124	-0.165	-0.126	0.127	-0.166	-0.13
	(0.1)	(0.13)	(0.28)	(0.11)	(0.13)	(0.28)
GDP	-0.0434	0.196***	0.374*	-0.0444	0.197***	0.376*
	(0.061)	(0.058)	(0.2)	(0.06)	(0.059)	(0.2)
$Temp_{Max35}$ × *fert*	-0.00379	0.00178	0.00401	-0.00386	0.00183	0.00407
	(0.0028)	(0.0034)	(0.0061)	(0.0028)	(0.0034)	(0.0062)
Industry	-0.994	0.669	-4.65	-1.01	0.68	-4.63
	(1.5)	(1.5)	(4.3)	(1.5)	(1.6)	(4.3)
Agriculture	-1.23	0.923	-0.374	-1.27	0.957	-0.282
	(2.8)	(2.5)	(5)	(2.7)	(2.5)	(5.1)
Pipe	0.0000146	0.00039	0.000597**	0.0000154	0.000375	0.0006**
	(0.00014)	(0.00036)	(0.00029)	(0.00014)	(0.00037)	(0.00029)
N	1140	876	991	1140	876	991
adj. R^2	0.409	0.430	0.481	0.411	0.428	0.481
BIC	1027	598	2132	1024	601	2132

Note: The coefficients are the regression results of the single-day high temperature models for DO, COD_{Mn}, and NH_3-N, representing the 100%-point effect on water quality per unit increase for a given temperature. '*twodays*', two consecutive days of highs above 35°C; '*threedays*', three consecutive days of highs above 35°C; '*fourdays*', four consecutive days of highs above 35°C; '$Temp_{Max35}$', the daily maximum air temperature; '*fert*' nitrogen application rate; '*GDP*', total GDP; '*Secondary*', the percentage of GDP output of the secondary sector; '*Primary*', the percentage of GDP output of the primary sector; '*Pipe*', length of drainage pipe; '*N*', the number of observations. Standard errors are clustered at the municipal level and are shown in parenthesis. (* $p < 0.1$, ** $p < 0.05$, *** $p < 0.01$.)

Supplementary Table 9. Continued.

	(7) DO	(8) COD_{Mn}	(9) NH_3-N
twodays			
threedays			
fourdays	-0.0794 (0.051)	0.0951^{*} (0.05)	0.0664 (0.11)
$Temp_{Max35}$	-0.865 (1.8)	-3^{*} (1.6)	-2.26 (2.1)
$Temp_{Max35}^2$	0.0132 (0.025)	0.0408^{*} (0.022)	0.0293 (0.029)
fert	0.137 (0.11)	-0.176 (0.13)	-0.138 (0.28)
GDP	-0.0432 (0.06)	0.199^{***} (0.059)	0.375^{*} (0.2)
$Temp_{Max35} \times fert$	-0.00418 (0.0028)	0.00208 (0.0034)	0.00431 (0.0064)
Industry	-1.02 (1.5)	0.781 (1.6)	-4.62 (4.3)
Agriculture	-1.3 (2.7)	1.04 (2.6)	-0.264 (5.1)
Pipe	0.0000133 (0.00014)	0.000359 (0.00037)	0.000602^{**} (0.00029)
N	1140	876	991
adj. R^2	0.411	0.430	0.481
BIC	1024	599	2132

Note: The coefficients are the regression results of the single-day high temperature models for DO, COD_{Mn} and NH_3-N, representing the 100%-point effect on water quality per unit increase for a given temperature. '*twodays*', two consecutive days of highs above 35°C; '*threedays*', three consecutive days of highs above 35°C; '*fourdays*', four consecutive days of highs above 35°C; '$Temp_{Max35}$', the daily maximum air temperature; '*fert*' nitrogen application rate; '*GDP*', total GDP; '*Secondary*', the percentage of GDP output of the secondary sector; '*Primary*', the percentage of GDP output of the primary sector; '*Pipe*', length of drainage pipe; '*N*', the number of observations. Standard errors are clustered at the municipal level and are shown in parenthesis. (* $p < 0.1$, ** $p < 0.05$, *** $p < 0.01$.)

Supplementary Table 10. Impacts of single-day high temperatures of Eq. (S8).

	(1) DO	(2) COD_{Mn}	(3) NH_3-N	(4) DO	(5) COD_{Mn}	(6) NH_3-N
$Temp_{Max35}$	-0.00527	-0.00559	-0.02	-0.607	-2.96*	-2.76
	(0.0042)	(0.0047)	(0.012)	(1.8)	(1.6)	(2.2)
$Temp_{Max35}^2$	-0.0000195	0.0000419	-0.000101	0.00963	0.0404*	0.0358
	(0.000092)	(0.00014)	(0.00023)	(0.025)	(0.022)	(0.029)
fert	-0.00147	-0.0343***	0.00146	0.12	-0.149	-0.107
	(0.0027)	(0.006)	(0.0083)	(0.1)	(0.13)	(0.28)
GDP	-0.0299*	0.0411	0.125*	-0.0402	0.195***	0.367*
	(0.018)	(0.068)	(0.064)	(0.06)	(0.059)	(0.2)
$Temp_{Max35} \times fert$	0.000195	-0.000194	0.000142	-0.00367	0.00138	0.00333
	(0.00012)	(0.00026)	(0.00046)	(0.0027)	(0.0034)	(0.0062)
Prec	-4.57*	-3.44*	-5.36	126**	-129*	-653***
	(2.6)	(1.9)	(4.6)	(62)	(75)	(218)
$Temp_{Max35} \times Prec$	0.12	0.122	0.179	-3.33*	3.69*	18.2***
	(0.12)	(0.08)	(0.19)	(1.7)	(2.1)	(6.2)
Industry	0.0654	0.983	0.688	-0.921	0.665	-4.33
	(0.72)	(1.3)	(2)	(1.5)	(1.5)	(4.4)
Agriculture	-2.16	1.4	4.56	-1.15	1	0.0596
	(1.6)	(1.9)	(3.4)	(2.8)	(2.5)	(5.1)
Pipe	-0.0000462	-0.0000909	0.0000795	0.0000167	0.000383	0.000585*
	(0.000037)	(0.00011)	(0.00011)	(0.00014)	(0.00036)	(0.00029)
N	60703	46239	48541	1140	876	991
adj. R^2	0.429	0.567	0.476	0.412	0.429	0.487
BIC	34690	53106	113575	1028	606	2125

285 **Supplementary Table 11. Results of the impacts for heatwave of Eq. (S10).**

	(1) DO	(2) COD_{Mn}	(3) NH_3-N	(4) DO	(5) COD_{Mn}	(6) NH_3-N
twodays	-0.044	0.0819*	0.00819			
	(0.05)	(0.042)	(0.099)			
threedays				-0.0888*	0.0207	0.0423
				(0.052)	(0.051)	(0.1)
fourdays						
$Temp_{Max35}$	-0.341	-3.5**	-2.81	-0.439	-2.87**	-2.34
	(1.9)	(1.6)	(2.2)	(1.8)	(1.1)	(2.1)
$Temp_{Max35}^2$	0.00607	0.0475**	0.0366	0.0075	0.0382**	0.0296
	(0.026)	(0.022)	(0.03)	(0.024)	(0.016)	(0.029)
fert	0.118	-0.153	-0.107	0.123	-0.24	-0.248
	(0.1)	(0.13)	(0.28)	(0.1)	(0.14)	(0.23)
GDP	-0.0403	0.195***	0.367*	-0.0412	0.193***	0.345*
	(0.061)	(0.058)	(0.2)	(0.06)	(0.065)	(0.18)
$Temp_{Max35}\times$	-0.00361	0.00149	0.00332	-0.00372	.00152	.00343
fert	(0.0027)	(0.0034)	(0.0061)	(0.0027)	(.0034)	(.0063)
Prec	125*	-126*	-653***	115*	-124*	-646***
	(62)	(70)	(219)	(63)	(72)	(218)
$Temp_{Max35}\times$	-3.28*	3.59*	18.2***	-3*	3.52*	17.9***
Prec	(1.7)	(1.9)	(6.2)	(1.7)	(2)	(6.2)
Industry	-0.953	.716	-4.33	-0.949	0.198	-3.62
	(1.5)	(1.5)	(4.4)	(1.5)	(1.7)	(5.7)
Agriculture	-1.14	1.06	0.0594	-1.17	0.0933	2.26
	(2.8)	(2.5)	(5.2)	(2.7)	(3.2)	(5)
Pipe	0.0000154	0.000386	0.000586**	0.0000164	0.000332	0.00041
	(0.00014)	(0.00036)	(0.00029)	(0.00014)	(0.00032)	(0.00029)
N	1140	876	991	1140	875	907
adj. R^2	0.412	0.431	0.487	0.414	0.367	0.510
BIC	1033	609	2132	1029	778	1857

286

Supplementary Table 11. Continued.

	(7) DO	(8) COD_{Mn}	(9) NH_3-N
twodays			
threedays			
fourdays	-0.0938*	0.0847	0.0601
	(0.053)	(0.053)	(0.1)
Temp_Max	-0.563	-2.99*	-2.77
	(1.8)	(1.6)	(2.2)
Temp_Max^2	0.00923	0.0407*	0.036
	(0.025)	(0.021)	(0.03)
fert	0.136	-0.164	-0.118
	(0.1)	(0.13)	(0.28)
GDP	-0.0398	0.198***	0.367*
	(0.06)	(0.059)	(0.2)
Temp_Max×fert	-0.0041	0.00177	0.00363
	(0.0028)	(0.0034)	(0.0064)
Prec	112*	-116	-642***
	(62)	(72)	(220)
Temp_Max× Prec	-2.91*	3.3	17.8***
	(1.7)	(2)	(6.2)
Industry	-0.962	0.808	-4.32
	(1.5)	(1.6)	(4.4)
Agriculture	-1.19	1.14	0.124
	(2.7)	(2.5)	(5.2)
Pipe	0.0000139	0.000358	0.00059**
	(0.00014)	(0.00037)	(0.00029)
N	1140	876	991
adj. R^2	0.414	0.430	0.487
BIC	1030	610	2131

Supplementary References.

Basu, N.B., Van Meter, K.J., Byrnes, D.K., Van Cappellen, P., Brouwer, R., Jacobsen, B.H., Jarsjö, J., Rudolph, D.L., Cunha, M.C., Nelson, N., Bhattacharya, R., Destouni, G. and Olsen, S.B. 2022. Managing nitrogen legacies to accelerate water quality improvement. Nat. Geosci. 15(2), 97-105.

Cahoon, L.B. and Hanke, M.H. 2019. Inflow and infiltration in coastal wastewater collection systems: effects of rainfall, temperature, and sea level. Water Environ. Res. 91(4), 322-331.

Cai, H., Mei, Y.D., Chen, J.H., Wu, Z.H., Lan, L. and Zhu, D. 2020. An analysis of the relation between water pollution and economic growth in China by considering the contemporaneous correlation of water pollutants. J. Clean Prod. 276, 13.

Chen, Y.F., Zhu, Z.T. and Cheng, S.Y. 2022. Industrial agglomeration and haze pollution: Evidence from China. Sci. Total Environ. 845, 11.

Hu, L.T., Meng, J., Xiong, C.Y., Fang, W., Yang, J.X., Liu, M.M., Bi, J. and Ma, Z.W. 2024. City-level resilience to extreme weather shocks revealed by satellite nighttime lights in China. Sust. Cities Soc. 101, 12.

Kotz, M., Wenz, L., Stechemesser, A., Kalkuhl, M. and Levermann, A. 2021. Day-to-day temperature variability reduces economic growth. Nat. Clim. Chang. 11(4), 319-U354.

Liu, K. and Lin, B.Q. 2019. Research on influencing factors of environmental pollution in China: A spatial econometric analysis. J. Clean Prod. 206, 356-364.

Ma, T., Sun, S., Fu, G.T., Hall, J.W., Ni, Y., He, L.H., Yi, J.W., Zhao, N., Du, Y.Y., Pei, T., Cheng, W.M., Song, C., Fang, C.L. and Zhou, C.H. 2020. Pollution exacerbates China's water scarcity and its regional inequality. Nat. Commun. 11(1), 9.

Pandit, M. and Paudel, K.P. 2016. Water pollution and income relationships: A seemingly unrelated partially linear analysis. Water Resour. Res. 52(10), 7668-7689.

van Vliet, M.T.H., Flörke, M. and Wada, Y. 2017. Quality matters for water scarcity. Nat. Geosci. 10(11), 800-802.

Vijay, R., Sardar, V.K., Dhage, S.S., Kelkar, P.S. and Gupta, A. 2010. Hydrodynamic assessment of sewage impact on water quality of Malad Creek, Mumbai, India. Environ. Monit. Assess. 165(1-4), 559-571.